Available online at www.sciencedirect.com
ScienceDirect
Scripta Materialia 59 (2008) 483–486
Scripta MATERIALIA
www.elsevier.com/locate/scriptamat

Mechanical behavior of open-cell metallic foams with dual-size cellular structure

D.P. Kou,[a] J.R. Li,[a,*] J.L. Yu[a] and H.F. Cheng[b]

[a] *CAS Key Laboratory of Mechanical Behavior and Design of Materials, University of Science and Technology of China, Hefei, Anhui 230026, China*

[b] *School of Material Science and Engineering, Hefei University of Technology, Hefei, Anhui 230009, China*

Received 7 March 2008; revised 10 April 2008; accepted 10 April 2008
Available online 25 April 2008

The mechanical properties of open-cell aluminum foams with dual-size cellular structure have been studied experimentally and numerically. Introducing secondary-size cells increases the stiffness and strength of open-cell aluminum foams. The effect of dual-size cellular structure optimization on the mechanical properties of open-cell foams is investigated using finite element analysis. Deformations of uniform-size and dual-size open-cell structures are compared and the mechanism whereby the dual-size cellular structure increases stiffness and strength is discussed.

Keywords: Open-cell metallic foams; Mechanical properties; Dual-size cellular structure; Finite element analysis; Microstructure optimization

During the last two decades metallic foams have been developed and are growing in use as new engineering materials. These ultralight metal materials possess unique mechanical properties, including high rigidity and large capacity to absorb impact energy. These properties are equal in all directions, and so the materials are tolerant to varying directions of loading, have a stable deformation mode and can adapt to loading conditions during deformation [1]. A number of processes have been developed to manufacture both open-cell and closed-cell metallic foams [2]. Of these, the infiltration method is used to produce open-cell aluminum foams. Common foams produced by the infiltration process display irregular cellular structures and their porosities vary from 60% to 70%. However, as recently reported by Despois et al. [3,4], a porosity of 88% could be achieved using this method by a replication technique. San Marchi and Mortensen [5] also produced open-cell foams with porosities ranging from 73% to 80%.

Although relative density has long been believed to be the dominating factor determining the stiffness and strength of foams [1], other parameters, such as cell packing, cell distribution and cell shape, might influence the mechanical behavior [6–8]. Li et al. [9] studied the effect.

The aluminum foams used in this study are made of commercially pure aluminum and manufactured by the infiltration method. Table 1 shows the parameters of the open-cell aluminum foams tested.

Cylindrical specimens 30 mm in diameter and 30 mm in height were prepared by wire cut electrical discharge machining and tested on an MTS810 testing system. A constant cross-head speed of 0.03 mm s^{-1} was used for all tests, corresponding to an initial strain rate of 10^{-3} s^{-1}, and strain was measured by dividing the cross-head displacement by the specimen height. For each type of aluminum foam, experiments were repeated at least twice. Because the results were reproducible, only one curve for each type of foam is presented.

The cellular structure of open-cell foams produced by the infiltration method is determined by the nature of the salt aggregate. San Marchi and Mortensen [5] have reported uniform-size open-cell aluminum foams. Cells were nearly spherically shaped and closely compacted (see Fig. 2 in Ref. [5]). Thereby, an idealized structure with cells that are spherical in shape and closely compacted in an fcc arrangement is assumed for simplicity in our numerical models, as shown in Figure 1a. Locations of secondary fillers are shown in Figure 1b. The distance between two adjacent centers of large fillers is a, the radii of large fillers and secondary fillers are R

* Corresponding author. Tel.: +86 551 3603044; fax: +86 551 3606459; e-mail: jrli@ustc.edu.cn

1359-6462/$ - see front matter © 2008 Acta Materialia Inc. Published by Elsevier Ltd. All rights reserved.
doi:10.1016/j.scriptamat.2008.04.022

Table 1. Parameters of open-cell aluminum foams

Type	Large filler size (mm)	Small filler size (mm)	f_s/f_l	ρ^*/ρ_s	E^* (GPa)	σ^* (MPa)
1	2.0	–	–	0.41	0.827	3.08
2	1.5	0.6	0.07	0.43	1.174	3.38
3	1.5	0.6	0.1	0.41	1.039	3.68
4	1.5	0.6	0.2	0.43	0.770	3.56
5	1.5	0.3	0.07	0.42	1.398	3.16
6	1.5	0.9	0.07	0.39	1.038	3.06

and r, respectively, and the volume fractions of large fillers and secondary fillers are f_l and f_s, respectively. If fillers contact each other normally, we have $R = a/2$, $r = (\sqrt{2}-1)R \approx 0.414R$ and $f_s \approx 0.071 f_l$. Overlap of fillers reduces the relative density of the cellular structures produced.

In our models, we consider six combinations of R and r, i.e. $r = 0.40R$, $r = 0.425R$, $r = 0.45R$, $r = 0.475R$, $r = 0.50R$ and $r = 0$ (the latter corresponds to uniform-size cells).

All finite element analyses are performed using the ABAQUS analysis package (Hibbit, Karlsson and Sorensen, Pawtucket, RI). A one-eighth unit cell is modeled owing to the cubic symmetry of fcc packing arrangement. C3D4 (four-node linear tetrahedron element) elements from the ABAQUS element library are used. After studying the mesh sensitivity, an element size of $0.014a$ was adopted as this is fine enough to obtain converged results. An isotropic material model with elastic–perfectly plastic stress–strain behavior is assumed in order to eliminate any dependence of the results on a chosen strain-hardening exponent. The Young's modulus E_s, Poisson's ratio v and yield stress σ_s are 70 GPa, 0.33 and 150 MPa, respectively.

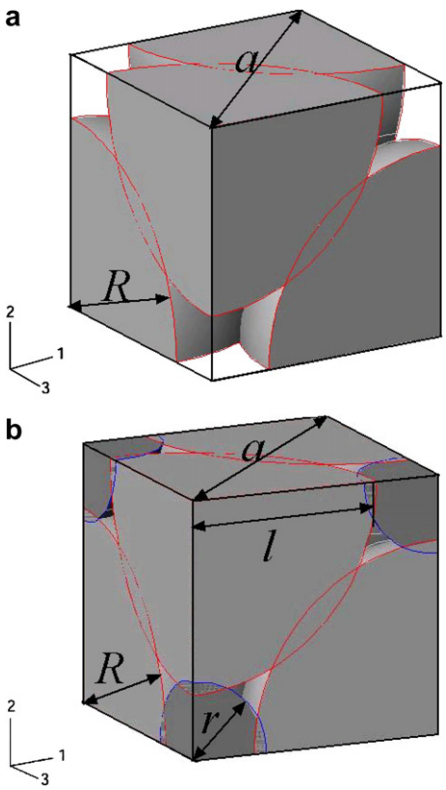

Figure 1. Compacted structures of fillers in open-cell arrangements: (a) uniform-size structure and (b) dual-size structure.

Symmetric boundary conditions are imposed on three surfaces of symmetry in the models. These include the bottom, the left and the front surfaces of the unit cell shown in Figure 1. The right and the back surfaces have periodic boundary conditions imposed. A displacement boundary condition is applied along the 2-direction on the upper surface. Reaction forces at the nodes of the displaced boundary are recorded and summed in order to compute the overall stress at each displacement increment. The Young's modulus of cellular structures is calculated at the first increment of simulations. The flow stress at 0.2% plastic deformation is chosen as the yield strength.

Compressive stress–strain curves of aluminum foams with different secondary cell fractions but identical secondary cell sizes ($r/R = 0.40$) are shown in Figure 2a. Stress–strain curves of dual-size foams with $f_s/f_l = 0.07$ and 0.10 are much higher than that of the uniform-size foam, while the stress–strain curve of dual-size foam with $f_s/f_l = 0.20$ is slightly lower than that of the uniform-size foam when strain exceeds 0.05, though the density of the dual-size foam is a little larger than that of the uniform-size foam. Compressive stress–strain curves of aluminum foams with the same secondary cell fraction ($f_s/f_l = 0.07$) but different secondary cell size are shown in Figure 2b. Stress–strain curves of all dual-size foams are higher than that of the uniform-size foam. The highest is the dual-size foam with $r/R = 0.4$. The initial stiffness E^* and flow stress at 0.2% plastic strain of all tested samples are listed in Table 1. This shows that, after introducing secondary cells, enhancements in stiffness and strength appear.

Figure 3a shows the dependence of the relative modulus E^*/E_s on the relative density of open-cell structures from finite element analysis. The stiffness increases remarkably with the introduction of secondary cells. The stiffness of dual-size cellular structures increases monotonously with the cell radius ratio r/R. Figure 3b shows the dependence of the relative strength σ^*/σ_s on the relative density of open-cell structures. The yield strength of all dual-size cellular structures increases considerably compared to that of uniform-size structures at equal density. Dual-size cellular structures with a cell radius ratio of 0.425 show the highest increase.

The dependence of the relative stiffness E_{dual}/E_0 and the relative strength σ_{dual}/σ_0 on the cell radius ratio r/R is shown in Figure 4, where E_{dual} and σ_{dual} are the stiffness and strength of dual-size cellular structures, while E_0 and σ_0 are the stiffness and strength of uniform-size cellular structures, respectively. The stiffness increases with increasing cell radius ratio in the range investigated, while the strength reaches a maximum when the cell radius ratio is 0.425. The effect is more prominent for structures with low density. For the dual-size cellular structure with a relative density of 0.18, a relative increase of 90% in stiffness and 60% in strength are achieved when the cell radius ratio is 0.425.

Comparison between the mechanical properties of cellular structures with variant densities and cell radius ratios suggests that improvements in mechanical

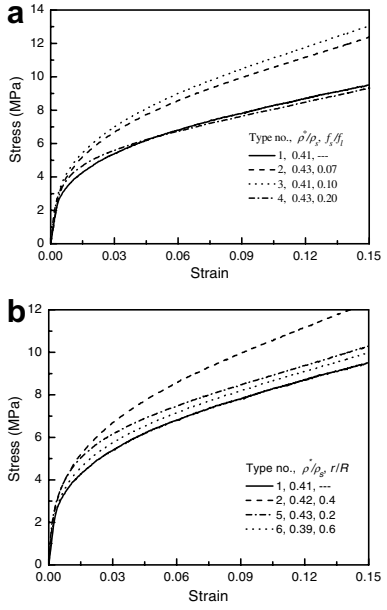

Figure 2. Compressive stress–strain curves of dual-size aluminum foams: (a) with different secondary cell fraction; (b) with different secondary cell size.

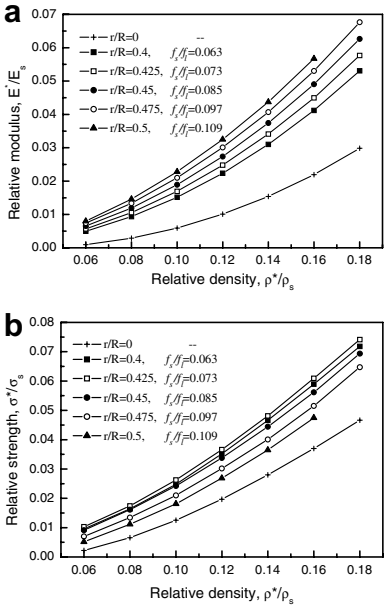

Figure 3. Mechanical properties of dual-size cellular structures: (a) relative modulus E^*/E_s vs. relative density ρ^*/ρ_s; (b) relative strength σ^*/σ_s vs. relative density ρ^*/ρ_s.

properties can be achieved by increasing the density or introducing secondary cells of a suitable size. Figure 5 shows the compressive stress–strain curves of four open-cell structures: the stiffness and strength of uniform-size cellular structures are highly improved when the relative density is increased from 0.1 to 0.14. However, by introducing secondary cells with a cell radius of $0.425R$, the mechanical properties of the dual-size cellular structure with a relative density of 0.1 are almost identical to those of the uniform-size cellular structure

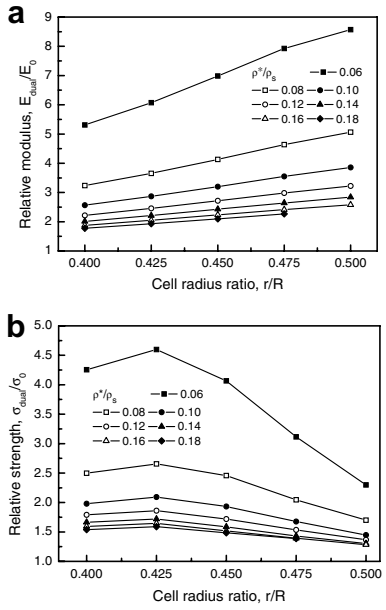

Figure 4. Mechanical properties of dual-size cellular structures: (a) relative stiffness E_{dual}/E_0 vs. cell radius ratio r/R; (b) relative strength σ_{dual}/σ_0 vs. cell radius ratio r/R.

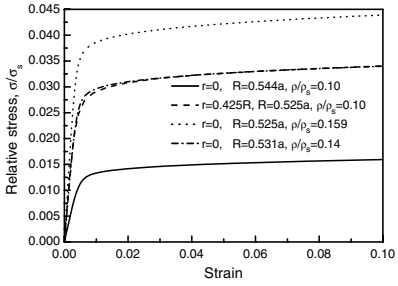

Figure 5. Compressive stress–strain curves of cellular structures with different values of r/R and relative densities.

with a relative density of 0.14. The response of the uniform-size cellular structure with $R = 0.525a$ and $\rho^*/\rho_s = 0.159$ is also presented for comparison.

Experimental results show that introducing secondary cells into open-cell foams improves the foam's mechanical performance. The dual-size open-cell aluminum foam with $r/R = 0.4$ and $f_s/f_l = 0.1$ shows the best strength, and its stiffness and strength are about 26% and 19% more than those of the uniform-size foam, respectively. The strength of the foam with $r/R = 0.4$ and $f_s/f_l = 0.07$ is slightly lower, and its stiffness and strength are about 42% and 10% more than those of the uniform-size foam, respectively. However, increasing f_s/f_l from 0.1 to 0.2 decreases the stiffness and strength. Furthermore, the mechanical properties of dual-size open-cell foams will degrade if the size of secondary cells exceeds the proper range. Smaller ($r/R = 0.20$) or bigger ($r/R = 0.60$) secondary cells are both not appropriate. Hence there is an optimal way to improve mechanical properties of open-cell foams by the dual-size cellular structure. Our experimental data indicates the proper size and volume fraction of secondary cells might be $r/R = 0.4$ and $f_s/f_l = 0.07$–0.1.

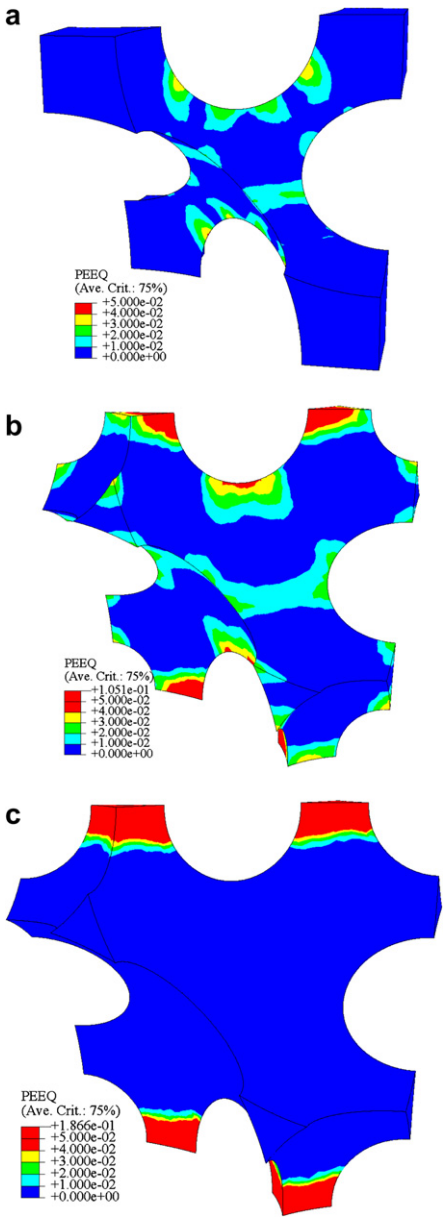

Figure 6. Equivalent plastic strain distributions in: (a) a uniform-size cellular structure; (b) a dual-size cellular structure with $r/R = 0.425$; and (c) a dual-size cellular structure with $r/R = 0.475$. The relative density is 0.1 and the compression strain is 2%.

In numerical simulations, the fcc packing structure with spherical cells is adopted. The relative density of computer models is less than 0.26. Among the five cell radius ratios ($r/R = 0.4$–0.5) we investigated, the stiffness increases monotonously with increasing r/R, while the strength shows a maximum increase at $r/R = 0.425$ (Fig. 4). The increases in stiffness and strength at a relative density of 0.18 could be as high as 90% and 60%, respectively. This indicates the optimal effect of secondary cells on the mechanical properties of open-cell structures.

The deformation behaviors of uniform-size and dual-size open-cell structures are different, as shown in Figure 6. For the uniform-size open-cell structure, plastic deformation is concentrated in major incline struts. Bending of the major incline struts is dominant. For the dual-size open-cell structure with $r/R = 0.425$, which has the optimal strength, plastic deformation disperses in both major struts and small struts. Further increasing the size of secondary cells, with $r/R = 0.475$, causes plastic deformation to accumulate in the vertical small struts and axial compression to become dominant. Comparing these three cases, introduction of secondary cells transforms material from plateau borders to major incline struts and strengthens the major incline struts. However, material transformation weakens the previous plateau border regions, and the small struts in those regions also contribute to the overall deformation. With further increasing r/R, more plastic deformation is shared by the vertical small struts. In the optimal condition of dual-size open-cell structures, both major incline struts and small struts almost equally share the deformation.

This work is supported by the National Natural Science Foundation of China (Projects Nos. 10302027, 90205003 and 10672156).

[1] L.J. Gibson, M.F. Ashby, Cellular Solids: Structure and Properties, second ed., Cambridge University Press, Cambridge, 1997.
[2] J. Banhart, Progress in Materials Science 46 (2001) U553–U559.
[3] J.F. Despois, R. Mueller, A. Mortensen, Acta Materialia 54 (2006) 4129–4142.
[4] J.F. Despois, A. Mortensen, Acta Materialia 53 (2005) 1381–1388.
[5] C. San Marchi, A. Mortensen, Acta Materialia 49 (2001) 3959–3969.
[6] A. Fazekas, R. Dendievel, L. Salvo, Y. Brechet, International Journal of Mechanical Sciences 44 (2002) 2047–2066.
[7] Z.J. Zheng, J.L. Yu, J.R. Li, International Journal of Impact Engineering 32 (2005) 650–664.
[8] T.G. Nieh, K. Higashi, J. Wadsworth, Materials Science and Engineering A–Structural Materials Properties Microstructure and Processing 283 (2000) 105–110.
[9] J.R. Li, H.F. Cheng, J.L. Yu, F.S. Han, Materials Science and Engineering A–Structural Materials Properties Microstructure and Processing 362 (2003) 240–248.